

$$G(t) = A \exp(-6D_2 t) + B G_{\text{int}}^{(1)}(t) \exp[-(D_1 + 5D_2)t] + C G_{\text{int}}^{(2)}(t) \exp[-(4D_1 + 2D_2)t], \quad (6)$$

with

$$A \equiv \frac{1}{4} (3 \cos^2 \theta - 1)^2,$$

$$B \equiv 3 \sin^2 \theta \cos^2 \theta,$$

$$C \equiv \frac{3}{4} \sin^4 \theta,$$

where  $\theta$  is the angle between the relaxation vector and the axis of the symmetric top,  $D_1$  is the rotational diffusion constant about the symmetry axis, and  $D_2$  is the rotational diffusion constant about an axis perpendicular to the symmetry axis.

If the internal rotation is treated by the extended diffusion model described above, the internal correlation functions are given by Eq. (1). Then, the overall reorientational correlation time defined as

$$\tau_c \equiv \int_0^\infty G(t) dt \quad (7)$$

can be evaluated in the reduced form to give

$$\tau_c^* = \frac{A}{6D_2^*} + \frac{B \tau_j^* F_1}{\tau_j^* - F_1} + \frac{C \tau_j^* F_2}{\tau_j^* - F_2}, \quad (8)$$

with

$$F_k \equiv \frac{1}{k} \sqrt{\pi/2} \exp(Y_k^2) \operatorname{erfc}(Y_k),$$

$$Y_k \equiv [\tau_j^{*-1} + 6D_2^* + k^2(D_1^* - D_2^*)] / k\sqrt{2},$$

and

$$D_\alpha^* \equiv \sqrt{I_\alpha/k_B T} D_\alpha, \quad \alpha = 1, 2.$$

This expression is valid over the entire range of  $\tau_j^*$  values and one can determine  $\tau_j^*$ 's from experimental values of  $\tau_c^*$  without any restriction on the range of validity.

In the internal rotational diffusion limit, the overall reorientational correlation time can be reduced to a more familiar expression as

$$\tau_c^* = \frac{A}{6D_2^*} + \frac{B}{D_1^* + 5D_2^* + \tau_j^*} + \frac{C}{4D_1^* + 2D_2^* + 4\tau_j^*}, \quad (9)$$

with  $\tau_j^*$  and  $4\tau_j^*$  the rotational diffusion limits of the internal correlation times according to Eq. (5). Also, in the internal free rotation limit,  $\tau_c^*$  can be readily reduced to

$$\tau_c^* = \frac{A}{6D_2^*} + B \sqrt{\pi/2} \exp[(D_1^* + 5D_2^*)^2/2] \operatorname{erfc}[(D_1^* + 5D_2^*)/\sqrt{2}] + C \sqrt{\pi/8} \exp[(4D_1^* + 2D_2^*)^2/8] \operatorname{erfc}[(4D_1^* + 2D_2^*)/\sqrt{8}]. \quad (10)$$

This expression can also be obtained from the beginning by introducing the Gaussian functions for the internal free rotational correlation functions in Eq. (6).

The above results may be applied to magnetic relaxation of a symmetric top molecule in liquid state to evaluate the internal correlation times and the degree of inertial effect.

- <sup>1</sup>W. A. Steele, *Adv. Chem. Phys.* **34**, 1 (1976); J. H. R. Clarke, *Adv. IR Raman Spectrosc.* **4**, 109 (1978).
- <sup>2</sup>D. E. Woessner and B. S. Snowden, Jr., *Adv. Mol. Relaxation Processes* **3**, 181 (1972).
- <sup>3</sup>H. W. Spiess, D. Schweitzer, and U. Haeberlen, *J. Magn. Reson.* **9**, 444 (1973).
- <sup>4</sup>T. E. Bull, *J. Chem. Phys.* **65**, 4802 (1976).
- <sup>5</sup>H. Versmold, *J. Chem. Phys.* **73**, 5310 (1980).
- <sup>6</sup>J. B. Lambert, R. J. Nienhuis, and R. B. Finzel, *J. Phys. Chem.* **85**, 1170 (1981).
- <sup>7</sup>M. A. Hamza, G. Serratrice, M.-J. Stebe, and J.-J. Delpuech, *Adv. Mol. Relaxation Int. Processes* **20**, 199 (1981).
- <sup>8</sup>P. Debye, *Polar Molecules* (Dover, New York, 1928); L. D. Favro, *Phys. Rev.* **119**, 53 (1960); K. A. Valiev, *Opt. Spectrosc.* **13**, 282 (1962).
- <sup>9</sup>D. Wallach, *J. Chem. Phys.* **47**, 5258 (1967).
- <sup>10</sup>D. E. Woessner, B. S. Snowden, Jr., and G. H. Meyer, *J. Chem. Phys.* **50**, 719 (1969).
- <sup>11</sup>H. Versmold, *J. Chem. Phys.* **58**, 5649 (1973).
- <sup>12</sup>R. G. Gordon, *J. Chem. Phys.* **44**, 1830 (1966).
- <sup>13</sup>R. E. D. McClung, *Adv. Mol. Relaxation Int. Processes* **10**, 83 (1977).

## Higher thermodynamic partial derivatives<sup>a)</sup>

Robert Gilmore

*Department of Physics and Atmospheric Science, Drexel University, Philadelphia, Pennsylvania 19104*  
(Received 9 March 1982; accepted 23 June 1982)

A simple algorithm was recently presented<sup>1</sup> for computing thermodynamic partial derivatives. This algorithm depends on the interpretation of the standard linear response functions (e.g.,  $C_p$ ,  $\alpha_p$ ,  $\beta_T$ ) as matrix elements of a linear susceptibility tensor. The algorithm is, therefore, valid only in the linear regime ("linear" algorithm), i.e., for the computation of first partial derivatives of thermodynamic variables and second partial derivatives of thermodynamic potentials.

The present work presents a simple "nonlinear" algorithm for computing higher thermodynamic partial derivatives (e.g.,  $\partial^2 V/\partial S \partial T$ ). The nonlinear algorithm depends only on one of the inputs to the linear algorithm and on an elementary theorem of calculus (chain rule). This theorem states that if  $x^i$ ,  $i = 1, 2, \dots, n$  and  $y^\alpha$ ,  $\alpha = 1, 2, \dots, n$  are two coordinate systems on a manifold (e.g., equation of state surface) at a point, the differentials  $dx^i$ ,  $dy^\alpha$ , and the partial derivatives

$\partial/\partial x^i$ ,  $\partial/\partial y^\alpha$  are related as follows:

$$dx^i = \sum_{\alpha=1}^n dy^\alpha J_\alpha^i, \quad (1d)$$

$$\frac{\partial}{\partial y^\alpha} = \sum_{i=1}^n J_\alpha^i \frac{\partial}{\partial x^i}. \quad (1p)$$

The linear algorithm is used to determine the linear transformation ( $n \times n$  matrix)  $J_\alpha^i = \partial x^i / \partial y^\alpha$ . To illustrate the nonlinear algorithm, we compute  $\partial^2 V / \partial S \partial T$  for a simple single-component fluid. The result will be expressed in terms of the linear response functions  $C_P$ ,  $\alpha_P$ ,  $\beta_T$ , and their first partial derivatives with respect to  $T$  and  $P$ .

(1) Identify the two independent coordinate systems. These are  $(x^1, x^2) = (T, -P)$  and  $(y^1, y^2) = (T, S)$ .

(2) Determine the linear relationship among the differentials  $(dT, -dP)$  and  $(dT, dS)$ . This is easily done using the linear susceptibility tensor

$$\begin{pmatrix} dS \\ dV \end{pmatrix} = \begin{pmatrix} C_P/T & V\alpha_P \\ V\alpha_P & V\beta_T \end{pmatrix} \begin{pmatrix} dT \\ -dP \end{pmatrix}. \quad (2)$$

The desired linear relationship is

$$\begin{pmatrix} dT \\ dS \end{pmatrix} = \begin{pmatrix} 1 & 0 \\ C_P/T & V\alpha_P \end{pmatrix} \begin{pmatrix} dT \\ -dP \end{pmatrix}. \quad (3i)$$

Inversion of this relation leads to

$$\begin{aligned} \begin{pmatrix} dT \\ -dP \end{pmatrix} &= \begin{pmatrix} 1 & 0 \\ C_P/T & V\alpha_P \end{pmatrix}^{-1} \begin{pmatrix} dT \\ dS \end{pmatrix} \\ &= \begin{pmatrix} 1 & 0 \\ -C_P/T & 1/V\alpha_P \end{pmatrix} \begin{pmatrix} dT \\ dS \end{pmatrix} \end{aligned} \quad (3ii)$$

and transposition leads to the desired linear relation of the form (1d):

$$(dT, -dP) = (dT, dS) \begin{pmatrix} 1 & -C_P/T \\ 0 & 1/V\alpha_P \end{pmatrix}. \quad (3iii)$$

(3) Use Eq. (1p) to obtain

$$\begin{pmatrix} \frac{\partial}{\partial T} \\ \frac{\partial}{\partial S} \end{pmatrix} = \begin{pmatrix} 1 & -C_P/T \\ 0 & 1/V\alpha_P \end{pmatrix} \begin{pmatrix} \frac{\partial}{\partial T} \\ -\frac{\partial}{\partial P} \end{pmatrix}. \quad (3iv)$$

(4) Compute:

$$\begin{aligned} \left(\frac{\partial}{\partial T}\right)_S V &= \left[ \left(\frac{\partial}{\partial T}\right)_P + \frac{C_P}{TV\alpha_P} \left(\frac{\partial}{\partial P}\right)_T \right] V \\ &= \left(\frac{\partial V}{\partial T}\right)_P + \frac{C_P}{TV\alpha_P} \left(\frac{\partial V}{\partial P}\right)_T \end{aligned}$$

$$= V\alpha_P - (C_P/T)(\beta_T/\alpha_P), \quad (3v)$$

$$\begin{aligned} \left(\frac{\partial}{\partial S}\right)_T \left[ \left(\frac{\partial V}{\partial T}\right)_S \right] &= -\frac{1}{V\alpha_P} \left(\frac{\partial}{\partial P}\right)_T \{ V\alpha_P - (C_P/T)(\beta_T/\alpha_P) \} \\ &= -\left(\frac{\partial}{\partial P}\right)_T \ln(V\alpha_P) \\ &\quad + \frac{1}{V\alpha_P} \left(\frac{\partial}{\partial P}\right)_T \left(\frac{C_P\beta_T}{T\alpha_P}\right). \end{aligned} \quad (3vi)$$

The following remarks are useful:

(1) This algorithm is applicable to systems described by any number of independent thermodynamic variables.

(2) This nonlinear algorithm includes the linear algorithm as a special case. This can be seen by comparing Eq. (3v) with the result of (3iv) in Ref. 1.

(3) Once the linear transformation (1p) between partial derivatives in the "new" and "old" coordinate system has been obtained, thermodynamic partial derivatives of arbitrary degree may be computed.

(4) Functions of thermodynamic variables [e.g.,  $\sigma = \sigma(T, P)$ ,  $\sigma = 0$  along a coexistence curve] can be chosen as independent variables. In the neighborhood of an equilibrium, a linear relationship exists between the differentials of the new and old variables (e.g.,  $d\sigma = -dP + mdT$ ). This linear relationship is used in Eq. (1d) to compute an expression for  $\partial/\partial\sigma$ .

(5) Partial derivatives involving one or more of the thermodynamic potentials among the independent variables may be computed using this algorithm. These calculations can be carried out by a variety of methods, including those described in Ref. 1.

(6) A partial description of the computation of higher thermodynamic partial derivatives has previously been given by Shaw.<sup>2</sup> This description extends only one degree beyond the linear regime (i.e., second derivatives of thermodynamic variables, third derivatives of thermodynamic potentials), is applicable only to simple single component substances described by two independent variables ( $n=2$ ), and depends extensively on tables. The present nonlinear algorithm suffers none of these defects.

(7) Shaw also tabulates partial derivatives of the form

$$\frac{\partial}{\partial w} \left[ \left(\frac{\partial x}{\partial y}\right)_r \right]. \quad (4)$$

The present algorithm can be used to compute partial derivatives of the form (4) by first applying the nonlinear algorithm to determine  $[\partial/\partial y, \partial/\partial z]$  in terms of a convenient set of partial derivatives (e.g.,  $\partial/\partial T, -\partial/\partial P$ ), followed by a second application of the algorithm to determine  $[\partial/\partial w, \partial/\partial r]$  in terms of the same convenient set of partial derivatives. In general, the nonlinear algorithm must be performed once for each new coordinate system introduced.

(8) This algorithm for computing partial derivatives beyond the linear response regime is applicable to any

physical system whose equation of state manifold is sufficiently smooth. In particular, it is applicable to nonequilibrium systems in the linear and nonlinear regimes.

<sup>a)</sup>Work supported in part by NSF Grant PHY810-2977.

<sup>1</sup>R. Gilmore, *J. Chem. Phys.* **75**, 5964 (1981).

<sup>2</sup>A. N. Shaw, *Philos. Trans. R. Soc. London Ser. A* **234**, 299 (1935).

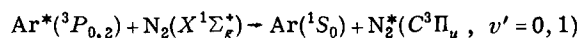
## Transfer of electronic excitation in collisions of metastable argon atoms with nitrogen molecules. II<sup>a)</sup>

C. R. Lishawa,<sup>b)</sup> W. Allison,<sup>c)</sup> and E. E. Muschlitz, Jr.

*Department of Chemistry, University of Florida, Gainesville, Florida 32611*

(Received 22 July 1982; accepted 9 August 1982)

The rotational state distributions in the product molecules for the process:



have been determined by spectroscopic observation of the fluorescent light ( $\text{N}_2^*, C \rightarrow B$ ) emitted at the intersection of supersonic molecular beams of the reactant species. Previous measurements of the  $v' = 0$  distributions have been reported.<sup>1</sup> These have now been repeated at relative collision energies of 0.161, 0.089, and 0.076 eV and extended to  $v' = 1$ .

The apparatus has been described in detail in the earlier paper.<sup>1</sup> The data collection system has been considerably improved, however, by the installation of a stepping motor to rotate the grating of the monochromator and the use of a multichannel scaler for storage of photon counts. The system is operated in synchronization with a mechanical chopper which interrupts the  $\text{N}_2$  beam. Background counts are subtracted for each chopper cycle and the resulting signal accumulated in a separate channel at each wavelength. This has made it possible to utilize longer counting times with subsequent increase in the precision of the results. The  $^3P_2$  and  $^3P_0$  states of Ar in the beam are assumed to be present in the statistical ratio of 5:1.

Figure 1 shows the measured band profiles (10 Å resolution) for the two C → B bands 0-0 and 1-0, at 0.161 eV relative kinetic energy. The vertical lines are the experimentally determined intensities with lengths appropriate to the standard error. The solid lines are computer generated spectra.<sup>2</sup> In the case of the 0-0 band, a Boltzmann distribution of the  $v' = 0$  rotational levels was found to give the best fit at all three relative energies. There is an overlap of the 1-1 band extending from about 3350 Å to lower wavelengths. In the computer generated spectrum, we assumed the previously measured<sup>1</sup>  $v' = 0/v' = 1$  population ratio 3.3 with a rotational population for  $v' = 1$  as determined from the analysis of the 1-0 band. In the case of the 1-0 band, the overlap of the 2-1 band is more serious and is responsible for the hump at 3135 Å. In generating the best fit to this spectrum we took the  $v' = 2/v' = 1$  popula-

tion ratio to be 60/290 as determined by Krenos and Bel Bruno,<sup>3</sup> and obtained a best fit to the rotational populations using a shifted Chebyshev polynomial series. The series was cut off after the third term, since the statistics indicated that no further information was gained by adding additional terms.

Figure 2 shows the population distributions obtained as described above. The dashed curves are "golden rule" calculations.<sup>1</sup> Arrows on the abscissae indicate the maximum  $J'$  allowed by conservation of energy. In the case of  $v' = 0$ , it can be readily seen that the golden rule greatly overestimates the rotational excitation as noted previously.<sup>1</sup> The "temperatures" corresponding to the rotational distributions obtained are 2200, 1600, and 1700 ± 100 K at 0.161, 0.089, and 0.076 eV. These

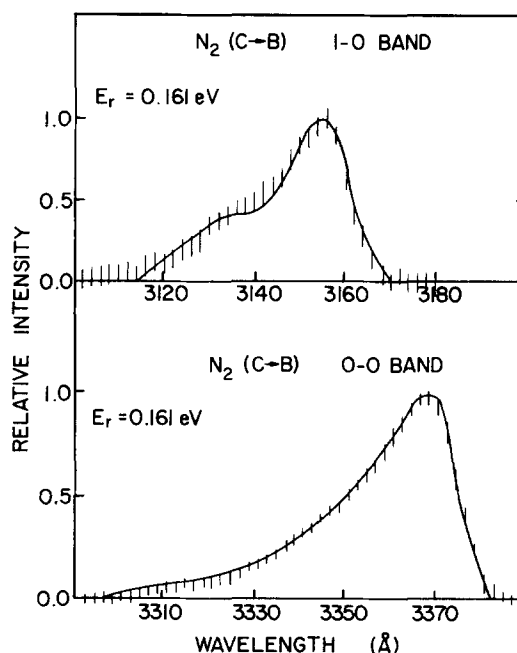


FIG. 1. Measured band profiles. The solid lines are computer-generated best fits to the data.